MINERALOGIA POLONICA
Vol. 9, No 1 — 1978

Leszek STOCH *, *Wanda S. SIKORA* *, *Leokadia BUDEK* *

MINERALOGY AND TECHNOLOGICAL PROPERTIES OF KAOLINITE SANDSTONES (SEDIMENTARY KAOLINS) FROM THE MARIA III DEPOSIT AT OŁDRZYCHÓW (LOWER SILESIA)

UKD 553.573:549.623.91:551.763.33:551.311.23+548.53:666.321(438-14) Ołdrzychów

A b s t r a c t. In the North-Sudetic Depression (Lower Silesia) there occur Santonian sandstones with the cement consisting of kaolinite and small amounts of micas and illite. The kaolinite shows a very high degree of crystallinity. By washing of sandstones, kaolin is obtained. It finds application in whiteware production, paper-making and other branches of industry. The paper presents detailed investigations of clay minerals occurring in these sandstones, as well as of the shape and size of their grains. The genesis of clay minerals is also discussed.

INTRODUCTION

The Maria III deposit situated at Ołdrzychów near Nowogrodziec (Jelenia Góra province) is mined for Santonian sandstones. These sandstones have a kaolinite cement with mica admixture (sedimentary kaolins) and soak readily in water. When they are subjected to washing and other treatment, clay fraction is separated from quartz and washed kaolin, the s.c. Maria III kaolin, is obtained. It has a wide range of application, e.g. in whiteware and paper industries, as plastic and rubber fillers, etc.

The Maria III deposit of Santonian kaolinite sandstones is situated in a deep tectonic depression striking WNW—ESE, referred to as the North-Sudetic Synclinorium. It is filled with Carboniferous (Westphalian), Permian (Rotliegendes), Triassic (Buntsandstein, Muschelkalk) and Upper Cretaceous sediments. Santonian sediments, represented by clays and sandstones with clay and brown coal intercalations, constitute a major lithostratigraphic unit of the Cretaceous. The argillaceous sandstone series attain up to 400 m in thickness. These are brackish and deltaic deposits (Milewicz 1968) extending virtually throughout the Synclinorium.

* Academy of Mining and Metallurgy, Institute of Geology and Mineral Deposits, Cracow (30-059 Kraków, al. Mickiewicza 30).

In the geological profile of the Santonian of the Fore-Sudetic Synclinorium the following petrographic types of sediments can be distinguished:

— sandstones with a kaolinite cement with mica admixture,
— kaolinite clays with mica or illite admixtures,
— kaolinite-illite clays.

In the Suszki area the content of sandstones is about 40%, that of kaolinite clays — 40% and the content of kaolinite-illite clays — 20%.

The Santonian sediments show fairly distinct cyclic alteration of beds. Each cycle comprises fine-grained kaolinite-illite clays overlain by coarser-crystalline kaolinite clays with a mica or illite admixture and sandstones cemented with kaolinite with a mica admixture.

The Santonian kaolinite clays are exploited for the needs of ceramic industry in several mines (Janina, Bolko) located near Bolesławiec.

MINERALOGICAL COMPOSITION OF KAOLINITE SANDSTONES

The sandstones recovered from the Maria III deposit at Ołdrzychów are medium- or fine-grained. White concentrations of clay substance up to 0.5 mm in size have been noted between quartz grains. Due to this, the sandstones macroscopically bear resemblance to weathered arkose sandstones.

Microscopic examinations have revealed that the sandstones in question have fairly high porosity. They are made up of angular or sub-rounded quartz grains with concentrations of kaolinite in between. The bulk of kaolinite forms aggregates pseudomorphous after feldspars. Fairly common are large kaolinite aggregates (Phot. 1), similar to those found in primary kaolins, being the product of weathering of micas. Alongside of kaolinite, large muscovite flakes showing a high degree of kaolinization can be encountered.

Table 1

Chemical composition of kaolinite sandstones

Component	Content, weight %
SiO_2	83.41
TiO_2	0.22
Al_2O_3	11.01
Fe_2O_3	0.26
MnO	0.002
MgO	0.14
CaO	0.36
K_2O	0.27
Na_2O	0.02
loss on ignition	4.30

Quartz appears, as a rule, in the form of single grains; aggregates of fine grains are not too common. The majority of quartz grains extinguish uniformly; about 20% shows wavy or mosaic extinciton. Some grains contain tourmaline (Phot. 2) and occasionally cyanite or rutile inclusions.

Accessory minerals are represented mainly by tourmaline, but also single grains of zircon, rutile and sometimes sillimanite are present. Anatase is very scarce.

The average chemical composition of kaolinite sandstones from the Maria III deposit, calculated from the data of several authors, is given in Table 1.

Table 2

Grain-size distribution of kaolinite sandstone

D μm	Content of grains of Stokes diameters $<D$	D μm	Content of grains of Stokes diameters $<D$
2000	99.6	20	19.6
1020	99.2	15	18.7
750	97.3	10	17.5
490	92.5	8	16.7
300	80.5	6	15.8
102	30.3	5	14.7
60	23.6	4	13.7
40	22.4	3	13.0
30	20.9	2	11.4
25	20.7		

The grain-size distribution of sandstones is shown in Table 2 and Figure 1. For <60 μm fractions it was determined on a Sartorius sedimentation balance whereas for >60 μm fractions, using dry sieve method. It has been found that sandy fraction (>0.1 mm), which is fine-grained (average grain size 0.2 mm), makes up about 70 weight %. The content of silt fraction is very low, while <40 μm fraction constitutes about 22 weight % of sandstones.

In general, the grain-size distribution of sandstones in the deposit is constant; its variations are relatively insignificant although both coarse-grained sections, containing grit fraction, and fine-grained silt sections, rich in very fine-grained quartz, can be encountered locally.

By washing of kaolinite sandstones, washed kaolin is obtained of a chemical composition as shown in Table 3. Its mineralogical composition is as follows:

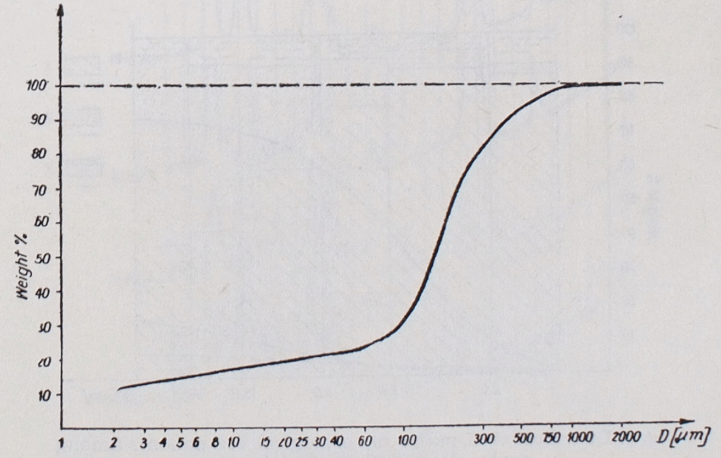

Fig. 1. Grain-size distribution of kaolinite sandstone

Table 3

Chemical composition of washed kaolin (KOC variety)

Component	Content, weight %	Component	Content, weight %
SiO_2	54.2	MgO	0.15
TiO_2	0.52	K_2O	0.60
Al_2O_3	32.18	Na_2O	0.07
Fe_2O_3	0.49	Loss on ignition	11.50
CaO	0.22		

Table 4

Content of representative chemical components of grain-classes of washed kaolin

Grain-class, μm	Content, weight %				
	total Fe_2O_3	soluble* Fe_2O_3	K_2O	Na_2O	loss on ignition 573—127 3K
>30	0.28	0.10	0.48	0.08	5.60
30—15	0.27	0.07	0.68	0.08	6.48
15—5	0.35	0.04	0.84	0.06	8.96
5—2	0.35	0.07	0.76	0.06	11.42
2—0,5	0.50	0.14	0.48	0.06	13.08
<0.5	1.16	0.47	0.84	0.06	12.80

* Mehra, Jackson (1960) — method.

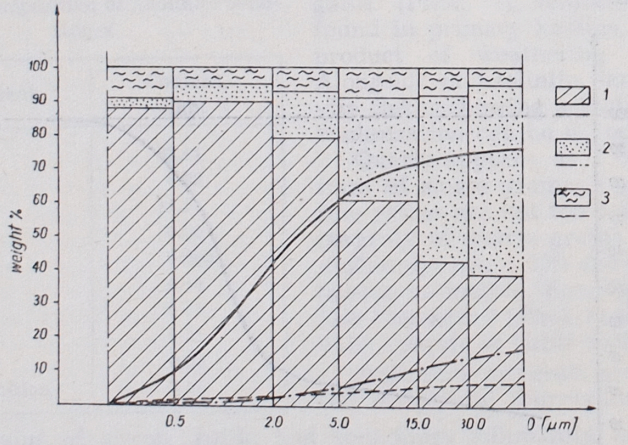

Fig. 2. Distribution of major mineralogical components among grain classes of washed kaolin
1 — kaolinite, *2* — quartz, *3* — micas

kaolinite 76 weight %,
muscovite + illite 7 weight %,
quartz 17 weight %.

The content of representative chemical constituents in grain classes of this kaolin is presented in Table 4 and their mineralogical composition in Table 5 and on a diagram (Fig. 2).

A feature deserving note is the relatively large size of kaolinite grains, most of which range from 0.5 to 15 μm in diameter (average grain size 1.6 μm). The content of micas is low, becoming somewhat higher in the range 2—30 μm, in which preserved muscovite grains and sericite concentrate. Below 0.5 μm the content of micas increases again because illite concentrates in this size interval. Illite yields a diffuse *001* line in X-ray diffraction patterns whereas this line produced by micas from coarser classes is very sharp (Fig. 3).

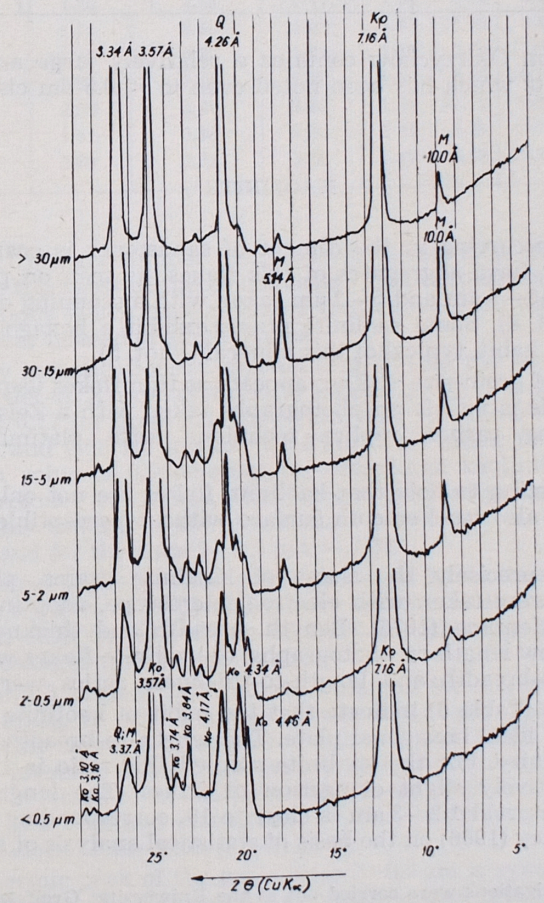

Fig. 3. Fragments of X-ray diffraction patterns of grain classes of washed kaolin

Table 5

Content of main mineralogical components in the grain — classes of washed kaolin

Grain-class, μm	Content of grain-class, weight %	Content of mineralogical components, weight %			Crystallinity index of kaolinite $I_{020} : I_{1\bar{1}0}$
		kaolinite	micas	quartz	
>30	4.7	39	5	56	not determined
30—15	6.9	43	8	49	not determined
15—5	16.5	61	9	30	0.77
5—2	27.3	79	7	14	0.68
2—0,5	34.8	90	5	5	0.62
<0.5	9.8	88	9	3	0.68

Kaolin from Ołdrzychów contains a relatively large amount of fine-grained quartz which has been noted even in < 0.5 μm class (Fig. 2, Table 3).

KAOLINITE

Kaolinite occurring in the cement of sandstones is coarse-crystalline. Above 2 μm it form aggregates of this flakes, as seen on photographs of grain glasses 15—5 μm and 5—2 μm taken with a scanning electron microscope (Phots 3, 4). Some kaolinite grains exhibit a hexagonal or pseudo-platesrhombic habit, typical of this mineral (Phot. 5).

Kaolinite of grain-size < 2 μm appears as thin flakes usually hexagonal in outline. This is visible on photographs taken with a Zeiss electron microscope, using carbon replica technique with platinum shadowing (Phot. 6) *.

It is interesting to note that kaolinite flakes are not only regular but, in most cases, also have smooth surface without perceptible growth steps or defects.

To define precisely the shape of kaolinite grains, photographs of < 2 μm class were taken with electron microscope, adopting a procedure proposed by Henning (1976). Length, breadth and thickness (the latter from the shadow length on photographs) of kaolinite flakes were measured. Also length-to-breadth and length-to-thickness ratios were determined.

The results (Table 6) indicate that the habit of kaolinite flakes resembles an almost ideal hexagonal plate. The length-to-breadth ratio for such plate equals unity. For the kaolinite studied this ratio is 1.3—1.4, which points to relatively slight elongation of flakes. The length-to-thickness ratio in size interval 1.2—3 μm is close to 10, corresponding to that determined by Conley (1966) on the basis of statistical analysis of kaolins. Flakes

* The investigations were carried out at the Uniwersitat Greifswald, Geologische Section.

Table 6

Size of kaolinite flakes < 2 μm

Grain-class	Medium length-L, μm	Medium breadth-B μm	Medium thickness-H μm	$\frac{L+B}{2}$	$\frac{L}{B}$	$\frac{L}{H}$	$\frac{B}{H}$	Content of grain-class, %
<0.2	0.14	0.10	0.02	0.12	1.31	6.20	4.71	39.86
<0.4	0.32	0.24	0.04	0.28	1.32	7.31	5.53	62.76
<0.6	0.57	0.42	0.08	0.50	1.32	6.77	5.09	74.75
<0.8	0.80	0.56	0.11	0.68	1.42	7.01	4.94	83.91
<1.0	1.03	0.74	0.14	0.88	1.38	7.07	5.10	89.76
<1.2	1.25	0.91	0.13	1.08	1.36	9.05	6.62	94.24
<1.4	1.52	1.06	0.16	1.29	1.43	9.35	6.49	96.39
<1.6	1.68	1.25	0.19	1.47	1.34	8.70	6.48	98.24
<1.8	2.11	1.21	0.18	1.66	1.73	11.53	6.63	98.52
<2.0	2.20	1.59	0.22	1.89	1.38	9.69	7.00	99.22
<2.4	2.51	1.85	0.34	2.18	1.35	7.28	5.38	99.61
<2.8	3.01	2.38	0.24	2.69	1.26	12.17	9.61	99.70
<3.2	3.55	2.61	0.38	3.08	1.35	9.23	6.79	99.90
<3.6	3.70	2.69	0.22	3.20	1.37	16.82	12.25	100.00

smaller than 1.0 μm are thinner (length-to-thickness ratio about 7). Above 3.5 μm average thickness of flakes increases. This is consistent with microscopic observations which have revealed that above 2 μm flake aggregates frequently appear instead of single flakes.

From X-ray investigations it appears (Fig. 3) that the structure of kaolinite is well ordered. X-ray crystallinity index $I_{020}/I_{1\bar{1}0}$ (Stoch, Sikora 1966) for kaolinite is 0.77 for grain size 15—5 μm, 0.68 for size 5—2 μm, 0.62 for size 2—0.5 μm and 0.68 for grains < 0.5 μm. This index for well ordered kaolinite has a value of 0.7 whereas for disordered kaolinite — 1.2—1.8. Due to the presence of quartz, Hincley's crystallinity index cannot be determined. This index for the grain class < 0.5 μm, virtually free of quartz, is 1.16 and for the class 2—0.5 μm — 1.34.

Thermal curves for respective grain classes of kaolinite show an endothermic peak at 843 K (570°C) and a very intense and sharp exothermic peak at 1253 K (980°C). The shape of DTA endothermic peak and DTG peak at 843 K changes with the grain size.

Figures 4 and 5 present DTA curves obtained for analyzed grain classes. It is interesting to note that for classes 30—15 μm and 15—5 μm the endothermic peak shows a prenounced inflexion at 953 K (680°C). This testifies to the presence of kaolinite with a higher dehydroxylation temperature, usually referred to as *kaolinite 700* (Hayes 1963; Keller 1966, 1967). This kaolinite is a common constituent of the Santonian clay sediments of the North-Sudetic Depression (Stoch 1978).

The endothermic peak of the grain class 2—0.5 μm is symmetrical, as in the case of well ordered kaolinite. An asymmetric kaolinite peak is yielded

by < 0.5 μm fraction. This change in the peak symmetry is due to the small size rather than the degree of crystallinity, which becomes obvious when thermal analysis is compared with X-ray investigations.

Data concerning the degree of ordering of the structure are also provided by infrared spectra. The intensity ratio of the 3692 cm^{-1} absorption band (stretching vibrations of free OH groups on the surface of octahedral sheet of the kaolinite layer) to the 3648 cm^{-1} band (vibrations of OH groups participating in interlayer hydrogen bonds) was assumed after Keeling (1963, 1965) as a measure of ordering. This ratio for kaolinite from different grain classes is as follows:

> 30 μm	2.14,
30—15 μm	1.84,
15— 5 μm	1.60,
5— 2 μm	1.52,
2—0.5 μm	1.82,
< 0.5 μm	2.17.

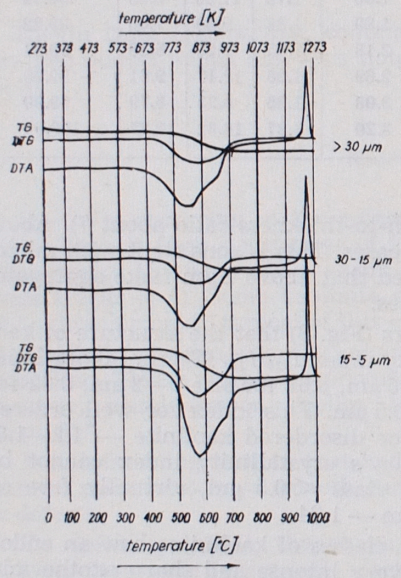

Fig. 4. Thermal curves for coarser grain classes of washed kaolin

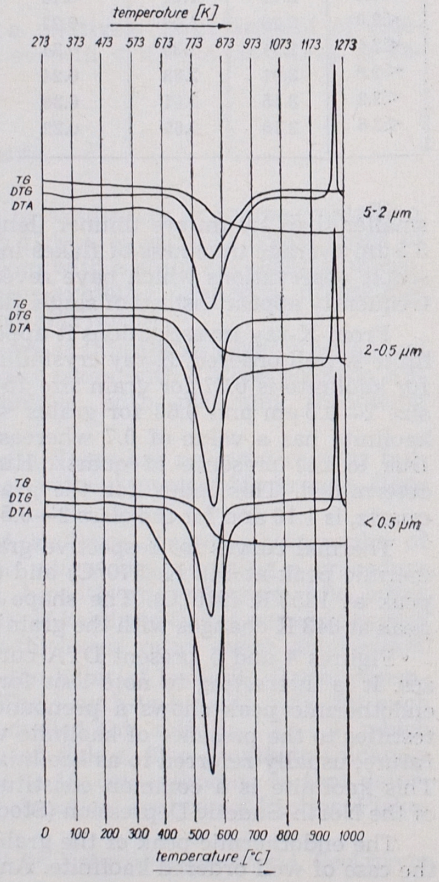

Fig. 5. Thermal curves for grain classes of washed kaolin (continued)

As can be seen, this index varies over a wide range, which is partly due to orientation of kaolinite flakes. It has been found that the intensity of some kaolinite absorption bands in the region close to 3600 cm^{1-} is sensitive to the degree of grain orientation. Nevertheless, the ratio has the lowest value in the size interval 15—2 μm. Both in finer and coarser classes, kaolinite shows a considerably lower degree of ordering of the structure. A similar trend has ben observed for X-ray crystallinity index.

MICAS

Inferences regarding the occurrence and nature of micas can be made on the basis of microscopic and X-ray investigations. Because of the small grain size, it was imposible to obtain an amount sufficient for detailed analysis. The intensity of the 10 Å line of micas in X-ray diffraction patterns of different grain classes shows substantial variability (Fig. 3).

Since feldspars are absent in the sandstones studied, there should be a correlation between the intensity of mica lines and potassium content. Such correlation failed to be noted in the analyzed grain classes because the intensity of the basal reflection of micas from different grain classes is affectted not only by the degree of their crystallinity but their chemical composition as well.

The mica line has the highest intensity in the grain class 30—15 μm, in which preserved non-kaolinized fragments of muscovite flakes are concentrated. In classes 15—5 μm and 5—2 μm sericite-type secondary micas are present, forming in the process of weathering of feldspars. Their basal reflections are much less intense. Fractions 2—0.5 μm and < 0.5 μm give very weak and diffuse basal lines. Illite-type fine-grained minerals of the mica group occur in these classes. From the diffuse 10 Å line it can be presumed that illite from < 0.5 μm class contains montmorillonite interstratifications.

IRON AND TITANIUM OXIDES

Mineral forms of iron and titanium oxides occurring in sandy fraction are different from those present in clay fraction. The contents of iron and titanium oxides, as well as the content of heavy minerals in grain classes coarser than 60 μm are given in Table 7.

Microscopic observation of heavy minerals separated from these classes in bromoform has revealed that sandy fraction (0.5—0.1 mm) contains a substantial amount of micas and tourmaline. Single grains of zircon, rutile and, sporadically, partly leucoxenized anatase have been identified. It is conceivable that sillimanite is present as well. This fraction also contains quartz with rutile inclusions. In silt fraction (0.1—0.6 mm) micas and tourmaline are less abundant whereas the content of zircon and rutile is fairly high. Anatase (Phot. 7) is relatively amply represented. Sporadic occurrences of sillimanite have been noted in this fraction as well.

Separation of heavy minerals from the sandy fraction results in a decresase in the content Fe_2O_3 and TiO_2 down to 0.037% and 0.042% respec-

tively. It follows therefore that heavy fraction is a carrier of about 50% Fe_2O_3 and 30% TiO_2. After it has been removed, the sandy fraction — on account of the content of colouring oxides — meets the requirements specified in raw material standards for good-quality glass-making sand.

Washed kaolin shows a different distribution of iron and titanium oxides (Table 4). Characteristic is the distribution of TiO_2 among respective grain classes (Fig. 6). Its content is higher in < 0.5 μm class, as well as in fractions coarser than 15 μm.

Titanium occurs in all the fractions, mainly in the form of anatase. The content of this mineral determined by X-ray method (Wiewióra 1970) in samples heated at 833 K (560°C) is given in Table 8. Anatase appears

Table 7

Content of colouring oxides and heavy minerals >60 μm

Grain-class, mm	Content, weight %		
	TiO_2	Fe_2O_3	Heavy minerals
>0.5	0.059	0.10	0.011
0.5—0.1	0.068	0.084	0.188
0.1—0.06	0.26	0.15	1.051

Table 8

Anatase content in grain-classes (determined by X-ray method)

Grain-class, μm	Content of anatase, weight %
>30	0.8
30—15	0.7
15—5	0.5
5—2	0.5
2—0.5	0.4
<0.5	1.0

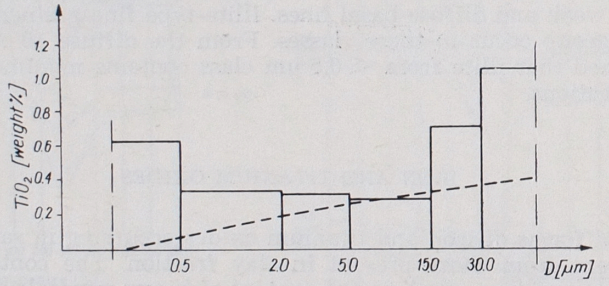

Fig. 6. Distribution of TiO_2 among grain classes of washed kaolin

in the form of well developed crystals, as can be seen on micrographs of this mineral separated from the clay fraction (Phot. 8). It can be presumed that anatase crystallized in situ, fixing titanium released during kaolinization of micas. It is feasible that TiO_2 occurs partly in the structure of micas. To determine the amount of TiO_2 fixed in micas, a method was adopted in volving studies of the kinetics of dissolution of wahed kaolin in 10% hydrofluoric acid. Figure 7 shows plots of the amount of K_2O, Fe_2O_3 and TiO_2 going into solution as a function of dissolution time. From potassium extraction curves it is evident that micas are completely dissolved already with in 30 h as after this time all potassium passes into solution.

After 30 h, a weak line at 10 Å can be observed in X-ray diffractogram of the undissolved residue, testifying to the presence of only a small amount of micas. Weak quartz reflections are also present, but the dominant mineral is anatase (lines 3.52, 2.42, 2.36, 2.33, 1.892, 1.698, 1.666 Å). Rutile lines have been recorded as well (3.25, 2.48, 2.20, 1.688, 1.620 Å). After a time longer than 30 h the rate of increase in TiO_2 concentration in the solution is very slow. This is because titanium originating only from dissolution of anatase and rutile goes into solution, and these minerals are considerably more chemically resistant. Extrapolating the straight line region of the curve corresponding to dissolution of anatase to the origin of coordinates, it can be read that 0.025% TiO_2 falls to micas. Remebering that the kaolin studied has a mica content of 7%, it has been calculated that micas contain about 0.36 wt. % of TiO_2.

Washed kaolin contains 0.44% Fe_2O_3. Iron distribution among individual grain classes is shown in Figure 8. The Fe_2O_3 content increases systematically with decreasing grain size. From the tech-

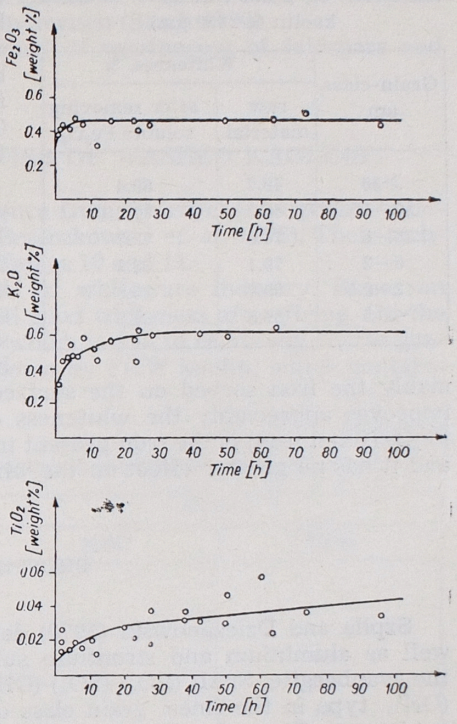

Fig. 7. Dissolution of TiO_2, K_2O and Fe_2O_3 from washed kaolin in 10% HF solution

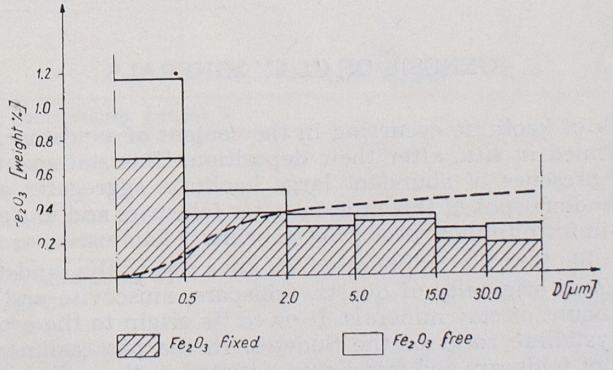

Fig. 8. Iron distribution among grain classes of washed kaolin

nological point of view, it is essential to know the content of chemically soluble iron because it is this iron that affects the whiteness of kaolin in raw state (Sikora 1974). To determine its content, the method of Mehra and Jackson (1960) was adopted, involving dissolution of iron oxides in sodium dithionite solution at pH about 7. Fine-grained iron oxides and hydroxides, as well as a part of iron adsorbed on the surface of kaolinite (free iron oxides) are dissolved. In this way, 0.17 wt. % of Fe_2O_3, i.e. 39% of its total content is removed.

Table 9

Whiteness of grain-classes of washed kaolin (λ=459 μm)

Grain-class, μm	Whiteness, %	
	raw material	after removing soluble Fe_2O_3
>30	49.7	69.4
30—15	68.3	72.2
15—5	74.0	77.7
5—2	79.1	83.5
2—0.5	80.7	85.8
<0.5	69.5	81.3

The content of soluble iron in respective grain classes is given in Table 4 and Figure 8. The finest classes show a high iron content. A rapid increase in its content with decreasing grain size, i.e. with increasing specific surface area of kaolinite, has been noted below 15 μm. It is presumably the iron sorbed on the surface of clay minerals and its removal improves appreciably the whiteness of kaolin (Table 9). The remaining Fe_2O_3 (fixed iron) is the iron present in the structure of micas or kaolinite, and it has no greater effect on the whiteness or raw kaolin (Sikora 1974).

PHOSPHATES

Szpila and Dzieżanowski (1978) detected basic lead and aluminium as well as aluminium and strontium sulphates and phosphate-sulphates of the svanbergite, $SrAl_3(PO_4)(SO_4)(OH)_6$, and hinsdalite, $PbAl_3(PO_4)(SO_4)(OH)_6$, type in the finest grain class of kaolin obtained from Ołdrzychów sandstones. They also contain barium (920 g/t), strontium (360 g/t), lead (420 g/t) and rare-earth elements (cerium, lanthanum).

GENESIS OF CLAY MINERALS

The bulk of kaolinite occurring in the cement of sandstones from Ołdrzychów formed *in situ*, after their deposition. This statement is supported by the presence of abundant large kaolinite aggregates and, specifically, of pseudomorphs of this mineral after feldspars and muscovite which are similar in form to those occurring in primary kaolins.

It is feasible that the sediment which gave rise to the sandstones in question consisted originally of quartz, feldspars, muscovite and possibly of a certain amount of clay minerals. It owed its origin to the erosion of weathering crystalline rocks of the Sudetes. In the post-sedimentary stage, weathering of feldspars and micas was initiated in the sediment. This process was promoted by intense infiltration of water through the porous sandy sediment. In consequence, feldspars were completely decomposed, muscovite nearly so, and substantial amounts of iron were removed.

The rise of well ordered kaolinite in the form of plates exhibiting a pseudohexagonal or nearly pseudohexagonal habit can be accounted for by recrystallization of fine-grained kaolinite that formed earlier or was brought with the sediment. Recrystallization of clay minerals in the post-sedimentation stage is a common phenomenon (Stoch 1977).

Illite is presumably also the product of weathering of feldspars and transformation of muscovite.

TECHNOLOGICAL PROPERTIES OF WASHED KAOLINS

By processing of kaolinite sandstones from Ołdrzychów, several varieties of washed kaolins are obtained (Brzęczkowski *et. al.* 1976). Their technological properties are presented in Tables 10 and 11.

The basic product is KOC kaolin for whiteware industry. It has an advantageously low Fe_2O_3 content and good whiteness after firing. On the other hand, its green strength is low, which is due to relatively coarse grain size. A higher green strength is shown by FKW kaolin, which contains

Table 10

Technological properties of kaolins for whiteware industry

Properties	Variety	
	KOC	FKW
Main chemical components, weight %		
Al_2O_3	32	32
Fe_2O_3	0.8	0.6
TiO_2	0.6	0.5
K_2O+Na_2O	0.8	1.0
Loss-on ignition	11	11
Content of grain-classes, weight %		
>60 μm	0.7	0.1
<5 μm	4.0	60
<2 μm	lack of data	54
Main mineral components, weight %		
Kaolinite	79	78
Quartz	13	13.5
Micas	7.5	8.5
Technological properties		
Whiteness (%) after firing at:		
1473 K (1200°C)	75	lack of data
1623 K (1350°C)	71	80
Green strength, kG/cm²	7.0	14.5
pH of suspension	lack of data	7

Table 11

Technological properties of kaolins for paper industry

Properties	Variety	
	FPW	FPP
Content of grain classes, weight %		
>63 μm	0.1	0.01
>10 μm	15.0	3.0
< 5 μm	60.0	9.6
< 2 μm	50.0	80.0
Main chemical components, weight %		
Al_2O_3	32.1	36.49
Fe_2O_3	0.50	0.46
TiO_2	0.49	0.49
Main mineral components, weight %		
Kaolinite	79	89.5
Micas	6	5
Quartz	17.4	5.5
Technological properties		
Whiteness, %	80	83
Green strenght, kG/cm²	4	lack of data
pH of suspension	5	6
Fe_2O_3 — soluble in HCl, weight %	<0.2	0.1

an addition of appropriately treated bentonite. It is also chemically bleached. The technological parameters of these two varieties are comparable with those of the Sedlec kaolin (Czechoslovakia).

FPW kaolin, used as filler, and fine-grained coating kaolin — FPP are intended for paper industry. Both varieties are chemically bleached. The technological properties of the latter are close to those of SPS kaolin manufactured by English China Clay.

Quartz grit, sand and silt obtained during the washing of kaolin are used as filter grit, glass-making sand, plastics fillers, etc. The sand and grit fractions are partly utilized by prefabricated-house factories.

DISCUSSION

The Santonian kaolinite sandstones mined from the Maria III deposit at Ołdrzychów near Bolesławiec (Lower Silesia) contain kaolinite in their cement. This kaolinite shows a high degree of crystallinity and occurs predominatly in the form of plates exhibiting a habit close to hexagonal. A part of kaolinite is characterized by a dehydroxylation temperature higher than normal (933 K or 650°C).

The kaolinite in question formed presumably during weathering processes operating in a porous sandy sediment that contained detrital feldspars and muscovite. Intense weathering and recrystallization led to the formation of the kaolinite peculiar to these sandstones.

From the Ołdrzychów sandstones washed kaolin, relatively low in Fe_2O_3 is obtained. Its content varies in respective grain classes, being the highest in the finest classes, particularly < 0.5 μm. Titanium oxide, appearing mainly as anatase, also concentrates in these grain classes.

A great part of Fe_2O_3 present in the kaolin, i.e. about 30% of its total content, is the iron adsorbed on the surface of kaolinite and that occurring in the form of fine-grained oxides (free Fe_2O_3). The remaining Fe_2O_3 occurs in the structure of micas (muscovite, sericite and particularly illite) and in kaolinite. The amonut of Fe_2O_3 in the structure of kaolinite is insignificant.

Washed kaolin obtained from the kaolinite sandstones of the North-Sudetic Depression finds application in whiteware production, paper-making and other branches of industry using mineral fillers (manufacture of plastics, rubber, etc.).

REFERENCES

BRZĘCZKOWSKI J., KOWALSKA J., PYTLIŃSKI A., 1976 — Kaoliny uszlachetnione ze złoża Maria III w Ołdrzychowie. *Geologia* Z. 23, 171—176.

CONLEY R. F., 1966 — Statistical distribution patterns of particle size and shape in the Georgia kaolins. *Proc. 14-th Nat. Conf.* 317—330.

HAYSS J. B., 1963 — Kaolinite from Warsaw Geodes, keokuk Region, Iowa. *Iowa Acad Sci.* 70, 261—272.

HENNIG K. H., 1976 — Elektronenmikroskopische Teilchengrössenanalyse von Kaoliniten. Schriftenr. geol. Wiss. 75—82.

HINCLEY D. N., 1963 — Variability in „Crystallinity" values among the kaolin deposits of the coastal plain of Georgia and South Carolina. *Clays Clay Miner.* 11, 229—235.

KEELING P. S., 1963 — Infra-red adsorption characteristics of clay minerals. *Trans. Brit. Ceram. Soc.* 62, 549—563.

KEELING P. S., 1965 — Investigation of hydroxyl groups in kaolinitic clays by infra-red spectrophometer. *Trans. Brit. Ceram. Soc.* 64, 137.

KEELER L. D., PICKETT E. F., REESMANN A. L., 1966 — Elevatet dehydroxylation termperature of the keokuk geode kaolinite a possible reference mineral. *Proc. Intern. Clay Conf.* 1.

KEELER L. D., 1967 — Elevatet dehydroxylation peak temperature of kaolinite. *Stone thermoscope* 1,1.

MEHRA O. P., JACKSON M. L., 1960 — Iron oxide removal from soils and clays by a dithionite-citrate system buffered with sodium bicarbonate. *Clays Clay Miner.* 7, 317—327.

MILEWICZ J., 1968 — The geological structure of the North-Sudetic Depression. *Biul. Inst. Geol.* 227, 5—31.

SIKORA W., 1974 — Żelazo w kaolinach pierwotnych Dolnego Śląska. *Pr. Miner.* 39.

STOCH L., SIKORA W., 1966 — Określenie stopnia uporządkowania struktury minerałów grupy kaolinitu. *Spraw. z Pos. Komisji Nauk. Oddz. PAN w Krakowie*, 651—654.

STOCH L., 1977 — Physico-chemical and structural aspects of the formation of clay minerals. *7-th Conf. on Clay Mineral. and Petrol. Karlovy Vary* 173—183.

STOCH L., 1978 — The occurrence of kaolinite 700° in some sedimentary rocks, its origin and properties (in press).

SZPILA K., DZIERŻANOWSKI P., 1978 — Minerały typu svanbergitu i hinsdalitu w kaolinach. *I Konf. Minerały i Surowce Ilaste.*

WIEWIÓRA A., 1970 — Tytan w kaolinie, w strukturze kaolinitu. *I Sympozjum Ceramiki i Surowców — Materiały* 41—48.

Leszek STOCH, Wanda S. SIKORA, Leokadia BUDEK

MINERALOGIA I WŁAŚCIWOŚCI TECHNOLOGICZNE PIASKOWCÓW KAOLINITOWYCH (KAOLINÓW OSADOWYCH) ZE ZŁOŻA MARIA III W OŁDRZYCHOWIE (DOLNY ŚLĄSK)

Streszczenie

Santońskie piaskowce kaolinitowe eksploatowane w kopalni Maria III w Ołdrzychowie koło Bolesławca (Dolny Śląsk), zawierają jako lepiszcze kaolinit o wysokim stopniu krystaliczności, wykształcony przeważnie w formie blaszek o pokroju bliskim heksagonalnemu. Część kaolinitu charakteryzuje się wyższą niż normalnie temperaturą dehydroksylacji (999 K tj. 650°C).

Kaolinit tworzył się przypuszczalnie w trakcie procesów wietrzeniowych przebiegających w porowatym osadzie piaszczystym, który zawierał detrytyczne skalenie i muskowit. Intensywne wietrzenie oraz procesy rekrystalizacji doprowadziły do utworzenia tak wykształconego kaolinitu stanowiącego ich specyfikę.

Z piaskowców tych otrzymywany jest kaolin szlamowany o stosunkowo niskiej zawartości Fe_2O_3. Jego udział jest różny w poszczególnych frakcjach ziarnowych; zwiększa się bardzo znacznie w klasach najdrobniejszych zwłaszcza $< 0{,}5$ μm.

Tlenek tytanu występujący głównie w formie anatazu również koncentruje się w tych klasach.

Duża część Fe_2O_3 występującego w tym kaolinie tj. około 30% jego ogólnej zawartości to żelazo zaadsorbowane na powierzchni kaolinitu oraz w postaci drobnoziarnistych tlenków (wolne Fe_2O_3). Reszta Fe_2O_3 występuje w strukturze mik (muskowit, serycyt) a zwłaszcza illitu. Ilość Fe_2O_3 w strukturze kaolinitu jest niewielka.

Kaolin szlamowany otrzymywany z piaskowców kaolinitowych niecki północnosudeckiej może być wykorzystywany w ceramice szlachetnej, w papiernictwie oraz innych przemysłach stosujących wypełniacze mineralne (produkcja tworzyw sztucznych, gumy itp.).

OBJAŚNIENIA FIGUR

Fig. 1. Rozkład wielkości ziarn piaskowca kaolinitowego
Fig. 2. Rozkład głównych składników mineralnych pomiędzy poszczególne klasy ziarnowe w kaolinie szlamowanym
1 — kaolinit, *2* — kwarc, *3* — miki
Fig. 3. Fragmenty dyfraktogramów frakcji ziarnowych kaolinu szlamowanego
Fig. 4. Krzywe termiczne grubszych klas ziarnowych kaolinu szlamowanego
Fig. 5. Krzywe termiczne drobniejszych klas ziarnowych kaolinu szlamowanego (c.d.)
Fig. 6. Rozdział TiO_2 pomiędzy klasy ziarnowe kaolinu szlamowanego
Fig. 7. Kinetyka rozpuszczania TiO_2, K_2O i Fe_2O_3 z kaolinu szlamowanego w 10% roztworze HF
Fig. 8. Rozkład żelaza pomiędzy poszczególne klasy ziarniste kaolinitu szlamowanego

OBJAŚNIENIA FOTOGRAFII

Fot. 1. Pseudomorfozy kaolinitu po mice, Pow. ×225
Fot. 2. Wrostki turmalinu w kwarcu, Pow. ×570
Fot. 3. Klasa ziarnowa 15—5 μm — mikroskop skaningowy. Pow. × 1000
Fot. 4. Klasa ziarnowa 5—2 μm — mikroskop skaningowy. Pow. × 1000
Fot. 5. Klasa ziarnowa 5—2 μm — mikroskop elektronowy. Pow. × 10 000
Fot. 6. Klasa ziarnowa < 2 μm — mikroskop elektronowy. Pow. × 12 600
Fot. 7. Minerały ciężkie z klasy ziarnowej 0,1—0,06 mm, 1 nicol. Pow. × 225:
A — anataz
Fot. 8. Anataz z kaolinu szlamowanego — mikroskop elektronowy. Pow. × 8400

Лешек СТОХ, Ванда С. СИКОРА, Леокадия БУДЭК

МИНЕРАЛОГИЯ И ТЕХНОЛОГИЧЕСКИЕ СВОЙСТВА КАОЛИНИТОВЫХ ПЕСЧАНИКОВ (ОСАДОЧНЫХ КАОЛИНОВ) В МЕСТОРОЖДЕНИИ МАРИЯ III В ОЛДРЖИХОВЕ (НИЖНЯЯ СИЛЕЗИЯ)

Резюме

Каолинитовые песчаники сантонского яруса добываются в шахте Мария III в Олдржихове вблизи Болеславца (Нижняя Силезия). Содержат они каолинит, который является цементом, с высокой степенью совершенства. В основном каолинит представлен пластинками с габитусом близким гексагональному. Часть каолинита отличается высшей, чем нормальная, температурой дегидроксилизации (999 K, т.е. 650°C).

Каолинит образовался предположительно во время процессов выветривания, которые проходили в пористом песчаном осадке, содержащим детритические полевые шпаты и мусковит. Интенсивное выветривание и процессы рекристаллизации привели к образованию каолинита, который является их результатом.

С этих песчаников получается отмученный каолин со сравнительно низким содержанием Fe_2O_3. Его содержание бывает разным в фракциях разного диаметра зёрн; значительно повышается в самых мелких фракциях, а особенно во фракции ниже 0,5 μм.

Окись титана, которая присутствует главным образом как анатаз, тоже концентрируется в этих фракциях.

Значительная часть Fe_2O_3, который содержится в этом каолине, т.е. около 30% его целого содержания, является железом адсорбированным на поверхности каолинита, а также в форме мелкозернистых окислов (свободный Fe_2O_3). Остальная часть Fe_2O_3 содержится в структуре слюд (мусковита, серицита), а особенно в иллите. Количество Fe_2O_3 в структуре каолинита незначительно.

Шламованный каолин, добытый из каолинитных песчаников северно-судетского бассейна, можно использовать в тонкой керамике, бумажной промышленности и в других отраслях промышленности, в которых используются минеральные заполнители (производство синтетиков, резины и т.п.).

ОБЪЯСНЕНИЯ К ФИГУРАМ

Фиг. 1. Распределение величины зерн каолинитового песчаника

Фиг. 2. Распределение основных минеральных составляющих в фракциях разного диаметра
1 — каолинит, *2* — кварц, *3* — слюды

Фиг. 3. Фрагменты дифрактограммов фракций зерна отмученного каолина

Фиг. 4. Термические кривые изучаемых фракций зёрн

Фиг. 5. Термические кривые изучаемых фракций зёрн (продолжение)

Фиг. 6. Распределение TiO_2 во фракциях

Фиг. 7. Кинетика растворения TiO_2, K_2O и Fe_2O_3 из отмученного каолина в 10% растворе HF

Фиг. 8. Распределение железа в фракциях разного диаметра

ОБЪЯСНЕНИЯ К ФОТОГРАФИЯМ

Фото 1. Псевдоморфозы каолинита на слюде. Увеличение × 225

Фото 2. Включения турмалина в кварце. Увеличение × 570

Фото 3. Фракция зерн 15—5 μм — сканнинг-микроскоп. Увеличение × 1000

Фото 4. Фракция зерн 5—2 μм — сканнинг-микроскоп. Увеличение × 1000

Фото 5. Фракция зерн 5—2 μм — электронный микроскоп. Увеличение × 10 000

Фото 6. Фракция зерн меньше 2 μм — электронный микроскоп. Увеличение × 12 600

Фото 7. Тяжёлые минералы из фракции 0,1—0,06 μм, 1 николь. Увеличение × 225
A — анатаз

Фото 8. Анатаз из шламованного каолина — электронный микроскоп. Увеличение × 8400

Phot. 1. Kaolinite pseudomorph after mica. Magn. × 225

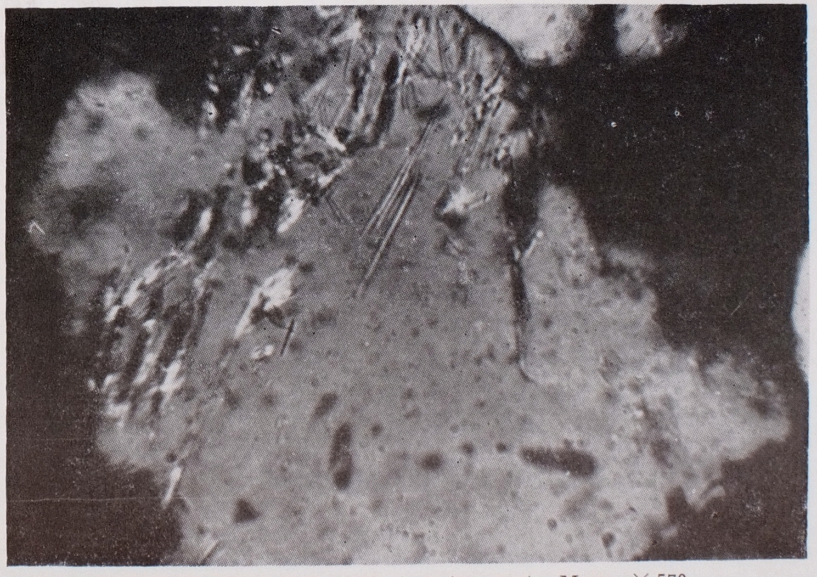

Phot. 2. Tourmaline inclusions in quartz. Magn. × 570

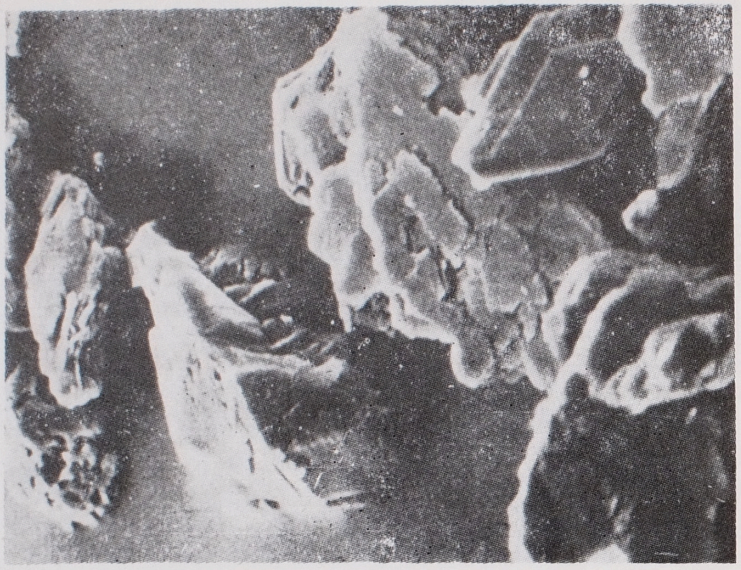

Phot. 3. Scanning electron microscope image — grain-class 15—5 μm. Magn. × 1000

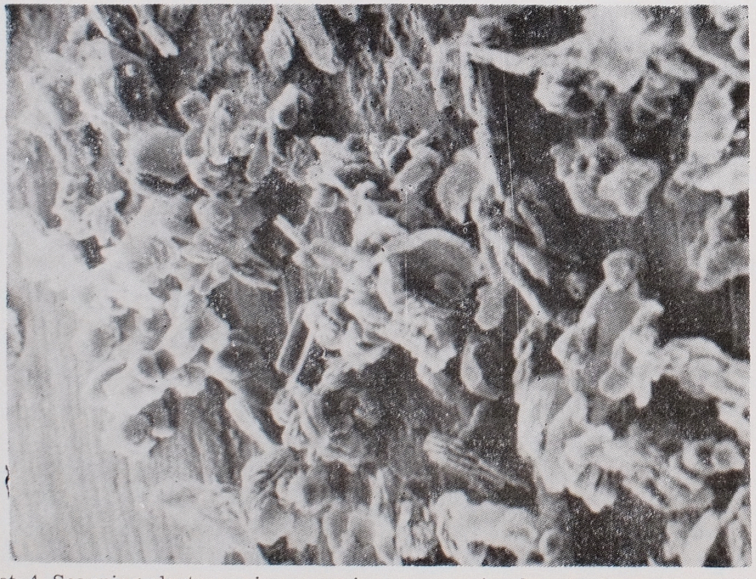

Phot. 4. Scanning electron microscope image — grain-class 5—2 μm. Magn. × 1000

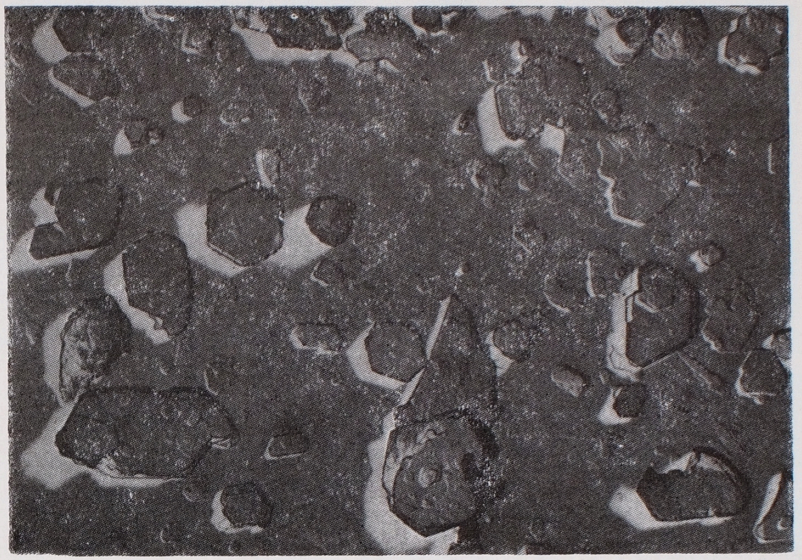

Phot. 5. Electron microscope image — grain-class 5—2 μm. Magn. × 10 000

Phot. 6. Electron microscope image — grain-class < 2 μm. Magn. × 12 600

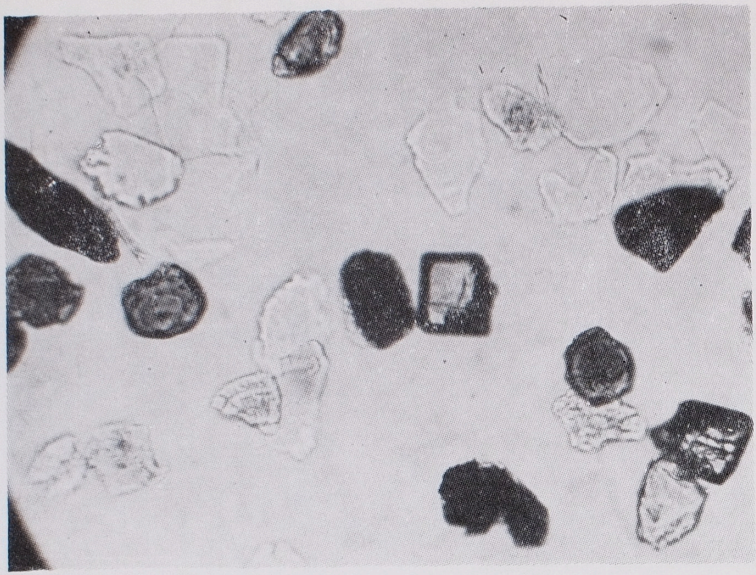

Phot. 7. Heavy minerals from grain-class 0.1—0.06 mm. 1 nicol. Magn. × 225
A — anatase

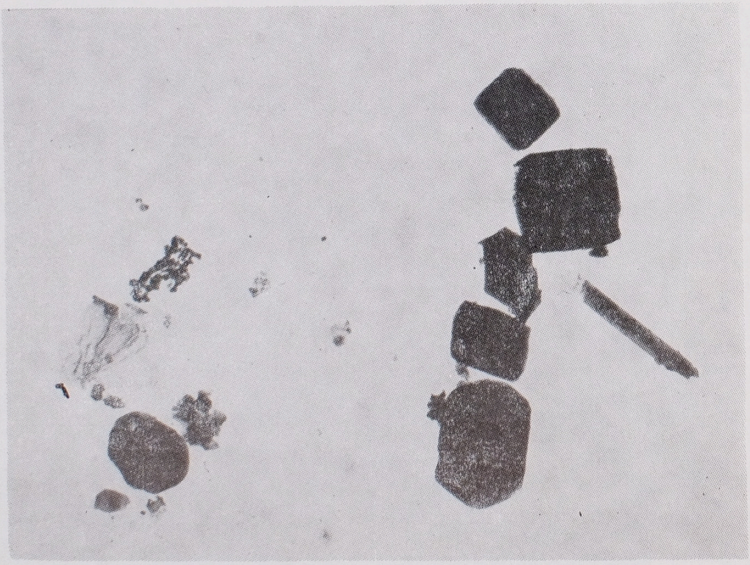

Phot. 8. Electron microscope image — anatase from washed kaolin. Magn. × 8400